A CRISPR-based genetic interaction map identifies synergistic drug combinations for cancer

Kyuho Han[1,4], Edwin E. Jeng[1,3,4], Gaelen T. Hess[1], David W. Morgens[1], Amy Li[1], & Michael C. Bassik[1,2,5]

[1] Department of Genetics, Stanford University, Stanford, CA 94305, USA

[2] Chemistry, Engineering, and Medicine for Human Health (ChEM-H), Stanford University, Stanford, CA 94305, USA

[3] Program in Cancer Biology, Stanford University, Stanford, CA 94305, USA

[4] Authors contributed equally

[5] Corresponding Author: bassik@stanford.edu

SUPPLEMENTARY TEXT

Analysis of the effect of two sgRNAs targeting the same gene on knockout efficiency

The CRISPR/Cas9 system has been shown to induce a spectrum of knockout alleles[1], which could complicate interpretation of genetic interactions. In addition, though it has been suggested that two sgRNAs targeting different locations within the same gene would synergistically enhance knockout efficiency[2], this has not been tested systematically. Since our system enables systematic analysis of genetic interactions between two sgRNAs, we looked closely at genetic interactions among double-sgRNAs targeting the same gene. As shown in supplementary figure 4, most of the pairs comprised of two sgRNAs targeting the same gene had buffering GIs. Interestingly, however, one of the top synergistic gene pairs predicted by GI_T score was TK1_TK1, a pair of the same genes (**Fig. 3d**). Therefore, when we systematically compared GIs of pairs of different sgRNAs targeting the same gene to those of the identical sgRNAs (**Supplementary Fig. 4a,b**), we observed more synergistic interactions from the pairs of the different sgRNAs. Although we observed buffering on average for most sgRNAs targeting the same gene, the pairs of the different sgRNAs showed less buffering - about half of the pairs of the identical sgRNAs (**Supplementary Fig. 4c**). Even for examples where a gene appeared to be synergistic with itself (**Supplementary Fig. 4d**), double-sgRNAs comprised of different sgRNAs were synergistic whereas double-sgRNAs comprised of identical sgRNAs were buffering. Overall, these data suggested that while most sgRNA pairs targeting the same gene show expected buffering, using two different sgRNAs to target different positions within the same gene could enhance the knockout efficiency. It has previously been shown that CRISPR-Cas9 system often produces functional in-frame variants[1]. The synergies we observed from some double-sgRNAs targeting the same genes might be explained by these in-frame variants: for example, each sgRNA might produce functional in-frame mutants with negligible single phenotypes, however, the double-sgRNA combined together could remove a large portion of the gene and cause synergistic phenotypic defect[3,4].

Comparison of the GI frequency of the DrugTarget CDKO map to GI frequencies measured in previously published GI maps

Many previous GI map studies support that genetic interactions are rare unless they are measured in a gene set enriched for related protein complexes or signaling pathways. For

example, one of the early yeast GI map studies from the Boone group[5] reported that the estimated frequency of synthetic lethal pairs was about 1 out of 200 (~0.5%). The most recent genome-by-genome yeast GI map from the same group[6] reported average GI frequency (considering both buffering and synergistic interactions) at 4.3%. A large 1376 x 72 gene Drosophila GI map by the Boutros group[7] reported a GI frequency of ~2.4% when using a growth phenotype. Finally, a 7 x genome-wide insertional mutagenesis screen in haploid human cells by the Brummelkamp group[8] found a total of 139 synthetic lethal interactions (~0.1%). To estimate GI frequency in our DrugTarget CDKO map, we calculated q-values (statistical significance in terms of false discovery rate) of genetic interactions based on the distribution of p-values[9] determined by the Mann-Whitney U test we used for GI_M scores (**see Supplementary Table 4 and 7**). When we used a q-value threshold of 0.05, the estimated GI frequency of the DrugTarget CDKO map is about 3.3%, which is comparable to previously reported GI frequencies.

SUPPLEMENTARY TABLES

Supplementary Table 1. Selected 207 genes for DrugTarget-CDKO library

Supplementary Table 2. 700 sgRNAs for DrugTarget-CDKO library

Supplementary Table 3. Distribution of double-sgRNAs per gene pair after filtering

Supplementary Table 4. GI scores of DrugTarget-CDKO screen

Supplementary Table 5. Selected 79 genes for Ricin-CDKO library

Supplementary Table 6. 284 sgRNAs for Ricin-CDKO library

Supplementary Table 7. GI scores of Ricin-CDKO screen

Supplementary Table 8. 246 STRING interactions between 79 Ricin hits

Supplementary Table 9. STRING interactions in the 66 most correlated gene pairs

Supplementary Table 10. Selected 79 genes for DrugTarget Batch-retest

Supplementary Table 11. 287 sgRNAs for DrugTarget Batch-retest

Supplementary Table 12. sgRNAs used for the validation of individual sgRNA pairs

Supplementary Table 13. Summary of sgRNA and drug validations

Supplementary Table 14. 30 most synergistic DrugTarget pairs

Figure S1.

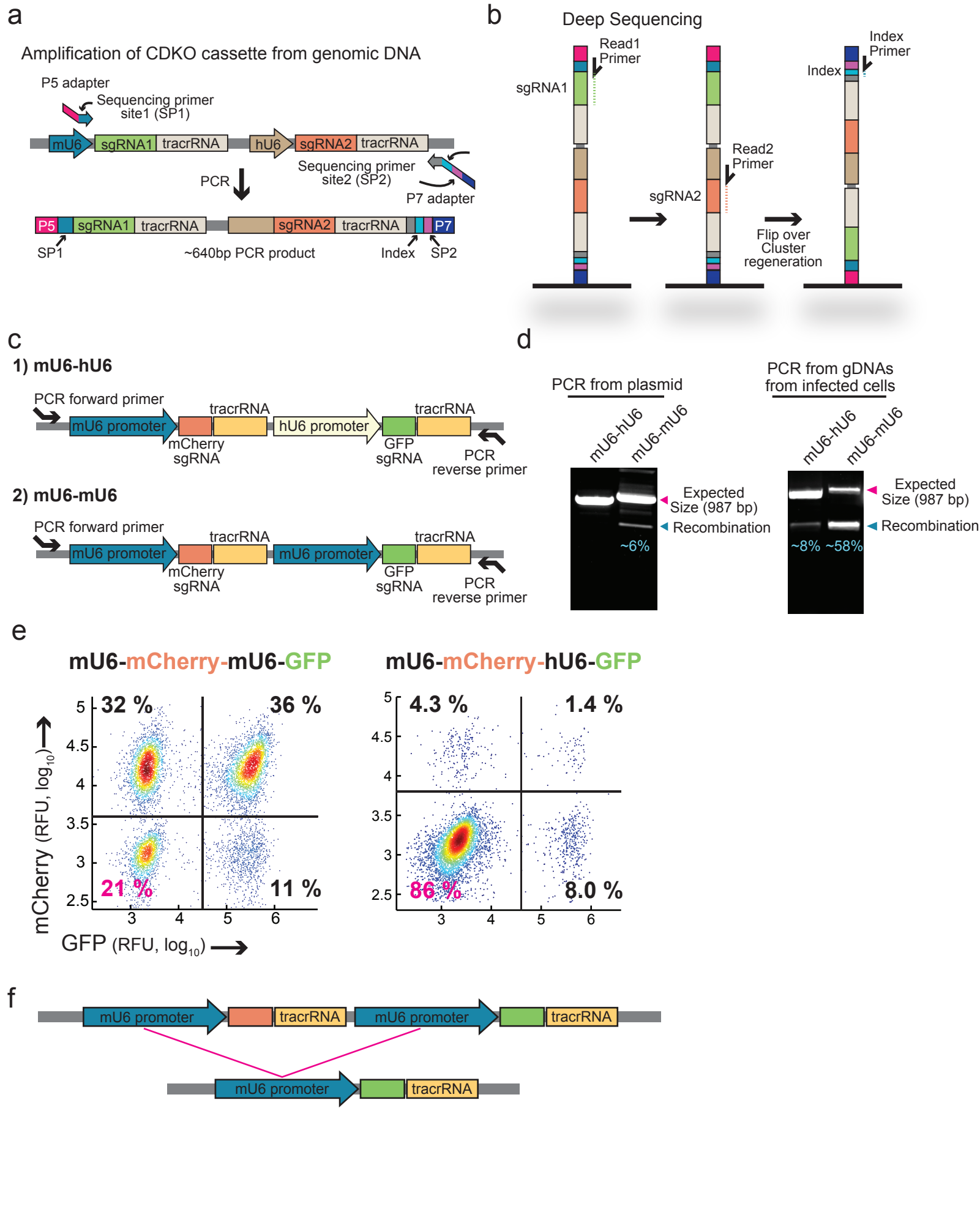
a
Amplification of CDKO cassette from genomic DNA
P5 adapter
Sequencing primer site1 (SP1)
mU6
sgRNA1
tracrRNA
hU6
sgRNA2
tracrRNA
Sequencing primer site2 (SP2)
PCR
P7 adapter
P5
sgRNA1
tracrRNA
sgRNA2
tracrRNA
P7
SP1
~640bp PCR product
Index
SP2
b
Deep Sequencing
Read1 Primer
sgRNA1
Read2 Primer
sgRNA2
Index Primer
Index
Flip over Cluster regeneration
c
1) mU6-hU6
PCR forward primer
mU6 promoter
tracrRNA
mCherry sgRNA
hU6 promoter
tracrRNA
GFP sgRNA
PCR reverse primer
2) mU6-mU6
PCR forward primer
mU6 promoter
tracrRNA
mCherry sgRNA
mU6 promoter
tracrRNA
GFP sgRNA
PCR reverse primer
d
PCR from plasmid
mU6-hU6
mU6-mU6
Expected Size (987 bp)
Recombination
~6%
PCR from gDNAs from infected cells
mU6-hU6
mU6-mU6
Expected Size (987 bp)
Recombination
~8%
~58%
e
mU6-mCherry-mU6-GFP
32 %
36 %
21 %
11 %
mU6-mCherry-hU6-GFP
4.3 %
1.4 %
86 %
8.0 %
mCherry (RFU, log10)
GFP (RFU, log10)
f
mU6 promoter
tracrRNA
mU6 promoter
tracrRNA
mU6 promoter
tracrRNA

Figure S1. A scalable CDKO system with minimized recombination compatible with deep sequencing

(a) Generation of PCR amplicons for deep sequencing (**see methods**). Double-sgRNA cassettes were directly amplified from genomic DNA and adapters were added during two rounds of PCRs. **(b)** Paired-end sequencing to directly read double-sgRNAs. PCR amplicons (around 640 bp) were clustered efficiently in flow cells and three custom sequencing primers used to read a front sgRNA, a rear sgRNA, and an index in order. **(c)** Double-sgRNA vectors with either two identical mU6 promoters, or mU6 and hU6 promoters driving expression of mCherry and GFP-targeting sgRNAs, were PCR-amplified using the primer pairs indicated. **(d)** The double-sgRNA cassettes in panel **c** were PCR-amplified from either purified plasmids or genomic DNA isolated from K562 cells infected with the corresponding double-sgRNA vectors. Expected size of the PCR amplicons are marked with red arrows and PCR amplicons from recombination-affected vectors are marked with blue arrows. **(e)** Flow cytometry analysis of GFP and mCherry knockout efficiency in cells infected with the vectors in panel. **(f)** Sequencing of the recombination-affected PCR amplicon from the double-sgRNA vector with two identical mU6 promoters shows that the recombination happens between two mU6 promoters.

Figure S2.

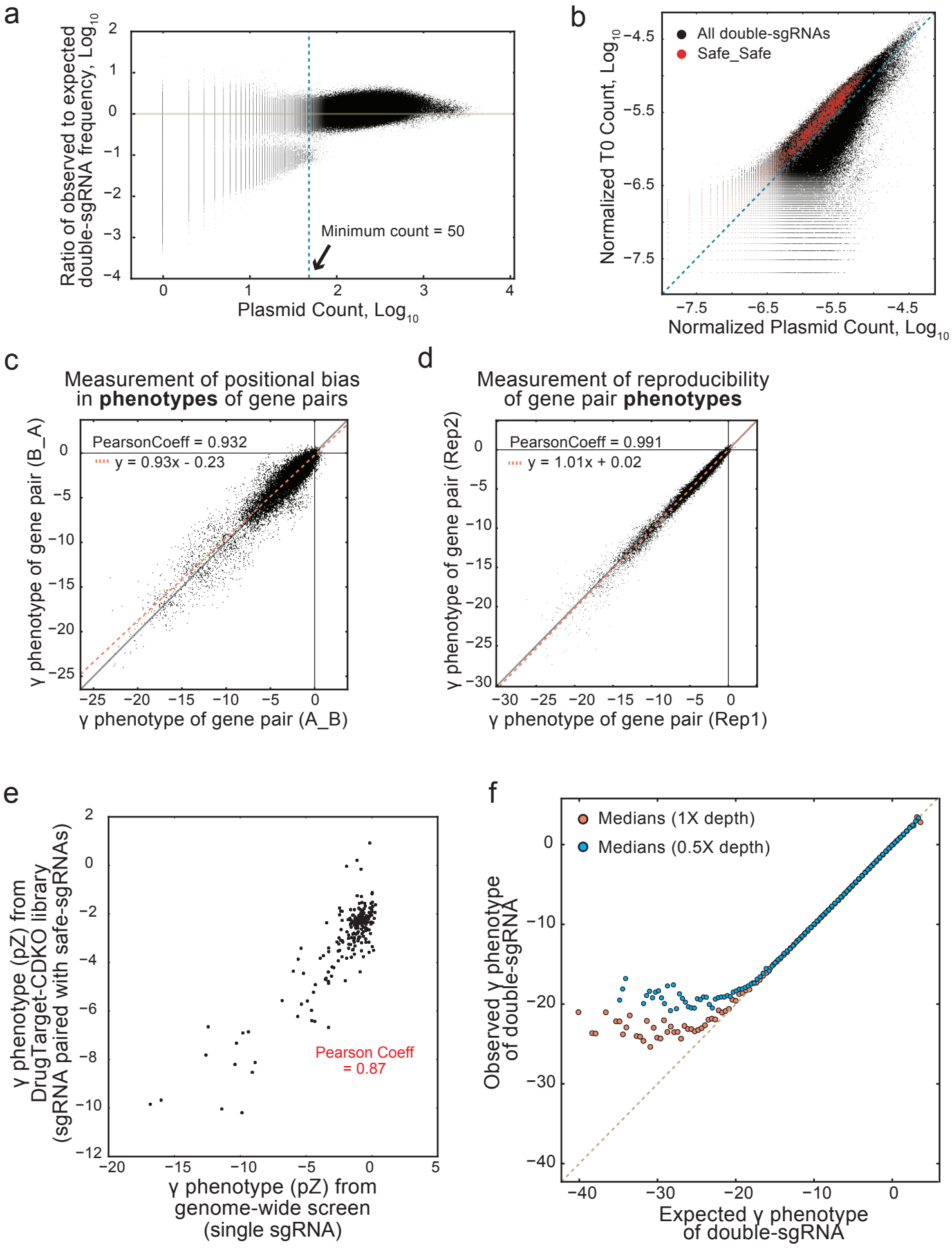
a
Ratio of observed to expected double-sgRNA frequency, Log10
Minimum count = 50
Plasmid Count, Log10
b
All double-sgRNAs
Safe_Safe
Normalized T0 Count, Log10
Normalized Plasmid Count, Log10
c
Measurement of positional bias in phenotypes of gene pairs
PearsonCoeff = 0.932
y = 0.93x - 0.23
γ phenotype of gene pair (B_A)
γ phenotype of gene pair (A_B)
d
Measurement of reproducibility of gene pair phenotypes
PearsonCoeff = 0.991
y = 1.01x + 0.02
γ phenotype of gene pair (Rep2)
γ phenotype of gene pair (Rep1)
e
γ phenotype (pZ) from DrugTarget-CDKO library (sgRNA paired with safe-sgRNAs)
Pearson Coeff = 0.87
γ phenotype (pZ) from genome-wide screen (single sgRNA)
f
Medians (1X depth)
Medians (0.5X depth)
Observed γ phenotype of double-sgRNA
Expected γ phenotype of double-sgRNA

Figure S2. Assessment of the DrugTarget-CDKO library quality

(a) Estimating the minimally required read count for a double-sgRNA. From the representation of single-sgRNAs in the hU6 and mU6 single-sgRNA library, the expected frequency of double-sgRNAs were calculated and compared to the observed frequency of double-sgRNAs in the DrugTarget-CDKO library. Ratios of the two frequencies showed that under ~50 read counts, the observed frequencies markedly fell below the expected. Based on this data, double-sgRNAs with less than 50 read counts were removed from further analyses. **(b)** Frequencies of double-sgRNAs were compared between the Plasmid library and the T0 sample. Frequencies of Safe_Safe sgRNAs were slightly enriched in the T0 sample since most double-sgRNAs have negative **γ** phenotypes. **(c)** Minimal positional bias in DrugTarget-CDKO library. **γ** phenotypes of gene pairs were compared between both orientations. **(d)** High reproducibility of measured **γ** phenotypes of gene pairs between two experimental replicates. **(e)** Single knockout phenotypes of genes are highly correlated between the DrugTarget-CDKO screen and a previous genome-wide single-sgRNA screen[10]. (**f**) Sequencing depth affects the phenotypic plateau observed in **Fig. 3a**.

Figure S3.

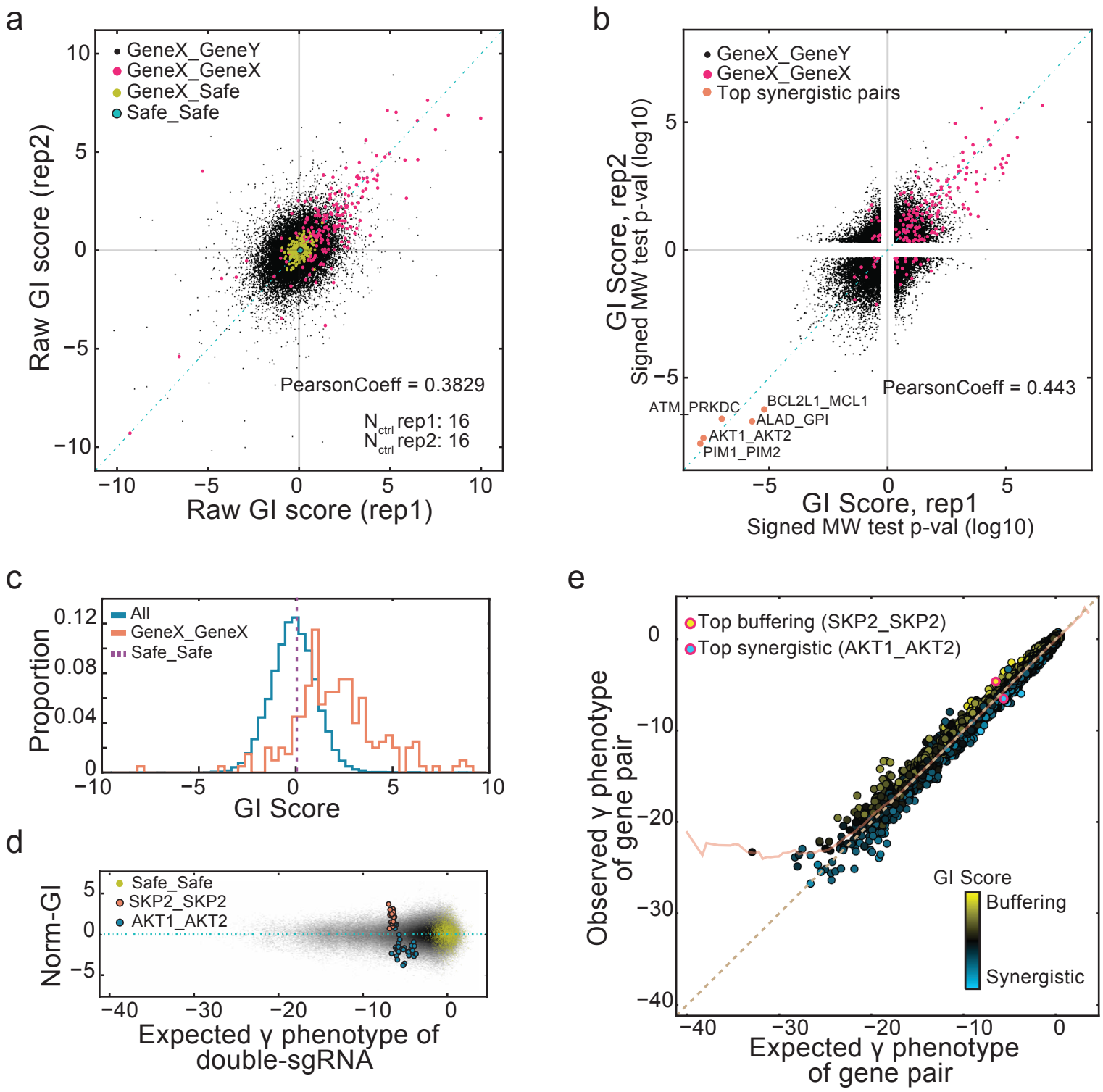
a
GeneX_GeneY
GeneX_GeneX
GeneX_Safe
Safe_Safe
Raw GI score (rep2)
Raw GI score (rep1)
PearsonCoeff = 0.3829
N_ctrl rep1: 16
N_ctrl rep2: 16
b
GeneX_GeneY
GeneX_GeneX
Top synergistic pairs
GI Score, rep2
Signed MW test p-val (log10)
GI Score, rep1
Signed MW test p-val (log10)
PearsonCoeff = 0.443
ATM_PRKDC
BCL2L1_MCL1
ALAD_GPI
AKT1_AKT2
PIM1_PIM2
c
All
GeneX_GeneX
Safe_Safe
Proportion
GI Score
d
Safe_Safe
SKP2_SKP2
AKT1_AKT2
Norm-GI
Expected γ phenotype of double-sgRNA
e
Top buffering (SKP2_SKP2)
Top synergistic (AKT1_AKT2)
Observed γ phenotype of gene pair
Expected γ phenotype of gene pair
GI Score
Buffering
Synergistic

Figure S3. Comparison of GI scores

(a) GI_T scores were calculated based on Raw-GIs and compared between two experimental replicates. **(b)** GI_M scores were calculated and compared between two experimental replicates (**see methods**). GI_M scores of gene pairs comprised of two same genes are marked in pink. The 5 most synergistic gene pairs are marked in orange. **(c)** Histograms of GI_T scores showed that most gene pairs comprised of two same genes are buffering (red solid line). GI_T score of Safe_Safe pair (purple dotted line). **(d)** Norm GIs of double-sgRNA combinations targeting the most synergistic (AKT1_AKT2) and most buffering (SKP2_SKP2) gene pairs by GI_T score were plotted against the expected **γ** phenotypes. These two pairs showed distinct GI distributions that were well-separated in opposite directions from 0. Safe_Safe double-sgRNAs are marked as yellow dots and all other double-sgRNAs are marked as grey dots. **(e)** Expected and observed **γ** phenotypes of gene pairs were plotted and color-coded by their GI_T score. The most synergistic (AKT1_AKT2) and buffering (SKP2_SKP2) pairs are highlighted.

Figure S4.

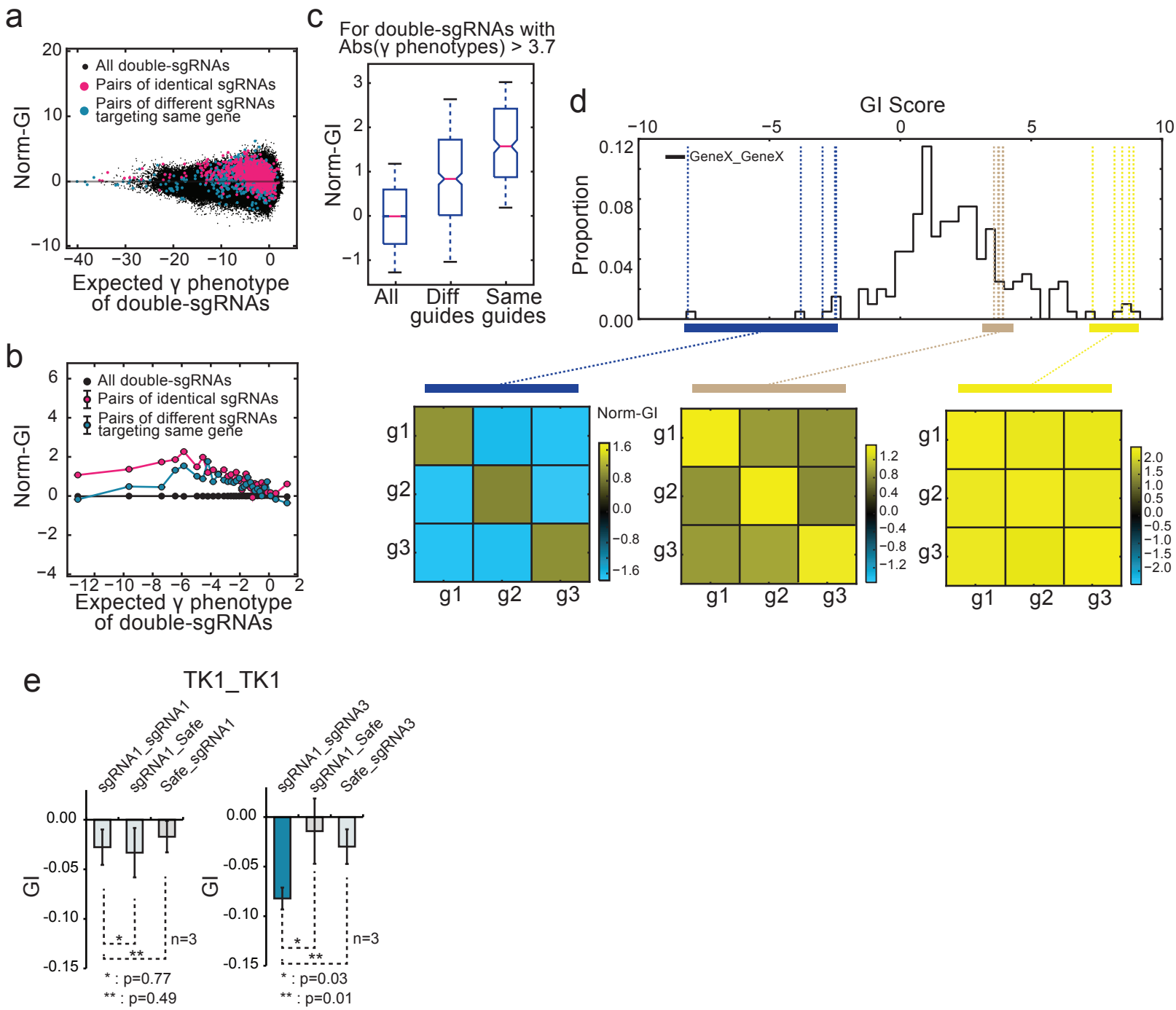
a
All double-sgRNAs
Pairs of identical sgRNAs
Pairs of different sgRNAs targeting same gene
Norm-GI
Expected γ phenotype of double-sgRNAs
b
All double-sgRNAs
Pairs of identical sgRNAs
Pairs of different sgRNAs targeting same gene
Norm-GI
Expected γ phenotype of double-sgRNAs
c
For double-sgRNAs with Abs(γ phenotypes) > 3.7
Norm-GI
All
Diff guides
Same guides
d
GI Score
Proportion
GeneX_GeneX
Norm-GI
g1
g2
g3

e
TK1_TK1
sgRNA1_sgRNA1
sgRNA1_Safe
Safe_sgRNA1
sgRNA1_sgRNA3
sgRNA1_Safe
Safe_sgRNA3
GI
n=3
* : p=0.77
** : p=0.49
* : p=0.03
** : p=0.01

Figure S4. Two different sgRNAs targeting the same gene are more synergistic than identical sgRNAs

(a-c) Norm-GIs were measured for three groups - all double-sgRNAs, pairs of same guides, and pairs of two different sgRNAs targeting the same genes. Two sgRNAs targeting the same gene tend to be buffering. However, two different sgRNAs targeting the same gene tend to be less buffering than two identical sgRNAs. **(a)** Norm-GIs were plotted against the expected **γ** phenotypes for all three groups (black: all double-sgRNAs, pink: double-sgRNAs comprised of two same guides, blue: double-sgRNAs comprised of two different guides targeting the same gene) **(b)** Plots in **a** were binned against the expected phenotype of double-sgRNAs. Data represent mean ± SEM. Data were binned in a way that each range includes at least 30 data points for any given group among the three. **(c)** Distribution of Norm-GIs for the three groups. Only double-sgRNAs with absolute **γ** phenotypes greater than 3.7 were analyzed. The pink line indicates the mean, the blue box represents the 25th-75th percentile, and the dotted bar indicates the 10th-90th percentile. **(d)** The Norm-GI patterns in 3 x 3 double-sgRNA combinations of pairs targeting the same gene. Top panel shows the distribution of GI scores for pairs targeting the same gene. The blue dotted lines mark the 5 most synergistic pairs in the distribution. The brown dotted lines represent the 35th-39th buffering pairs, and the yellow dotted lines mark the 5 most buffering pairs in the distribution. All double-sgRNA combinations for each group were averaged over the 3 x 3 grid and color-coded by their Norm-GIs. **(e)** In the dual sgRNA validation assay, two different sgRNAs targeting TK1 showed synergistic GI whereas two identical sgRNAs did not show significant GI. Data represent mean ± SD (n=3) fromreplicate cultures.

Figure S5.

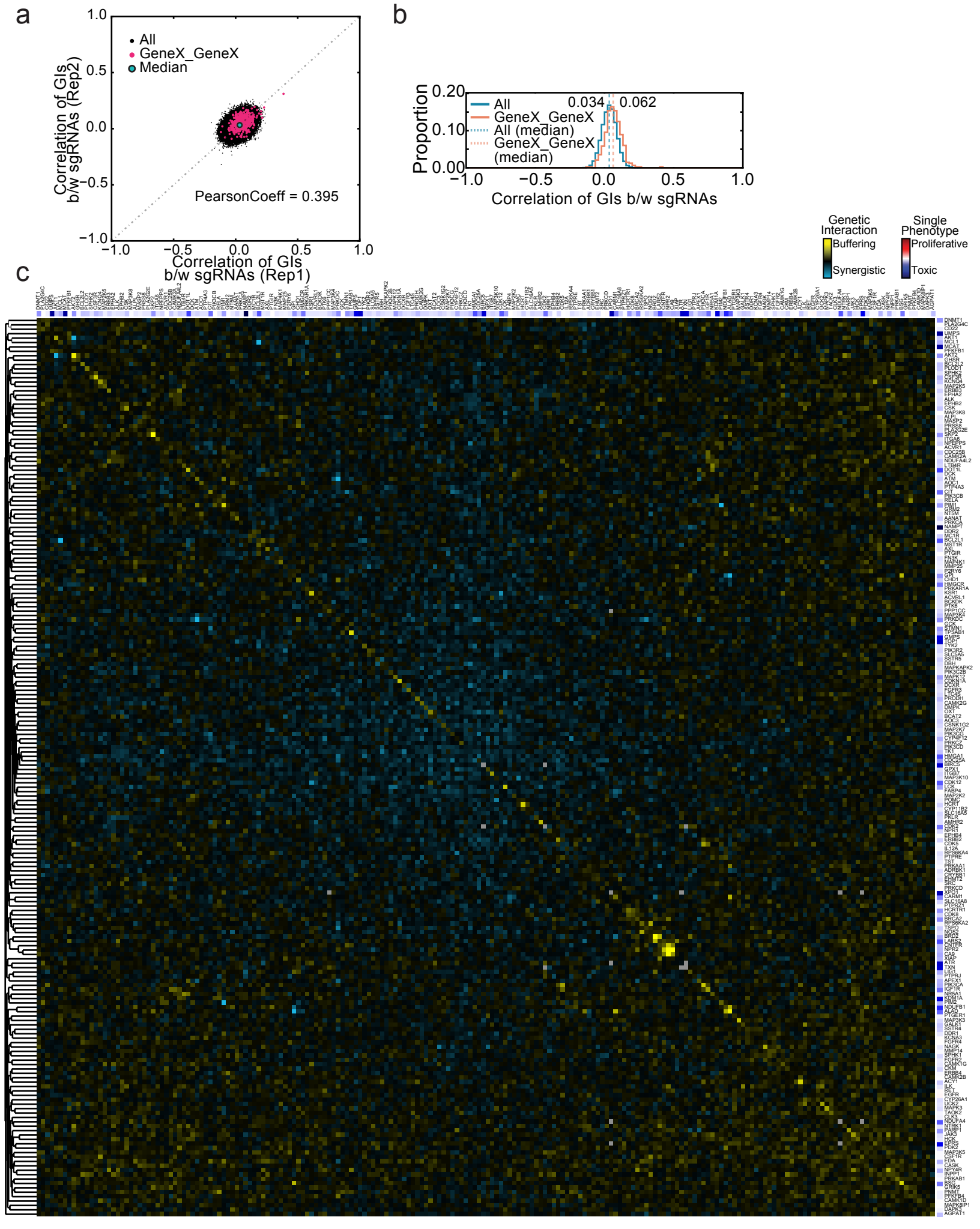
a
b
c
All
GeneX_GeneX
Median
PearsonCoeff = 0.395
Correlation of GIs b/w sgRNAs (Rep1)
Correlation of GIs b/w sgRNAs (Rep2)
All
GeneX_GeneX
All (median)
GeneX_GeneX (median)
0.034
0.062
Proportion
Correlation of GIs b/w sgRNAs
Genetic Interaction
Buffering
Synergistic
Single Phenotype
Proliferative
Toxic

Figure S5. γ phenotype-based DrugTarget-CDKO GI map shows sparse genetic interactions

(a) Correlations of GI profiles between two sgRNAs were compared in two experimental replicates: sgRNAs targeting the same gene are marked in pink. Due to the low GI frequencies, correlations of GI profiles between sgRNA pairs were very low. **(b)** The distributions of correlations of GI profiles for all sgRNA pairs (blue) and for sgRNAs pairs targeting the same gene (orange). Medians of the distributions are marked by dotted lines. **(c)** Sparse genetic interactions in the DrugTarget-CDKO GI map. GI_M scores of all gene pairs were calculated and color-coded by a yellow-cyan heatmap. Genes were hierarchically clustered by their correlation of GI profiles. **γ** phenotypes of individual genes are marked in sidebars with a red-blue heatmap.

Figure S6.

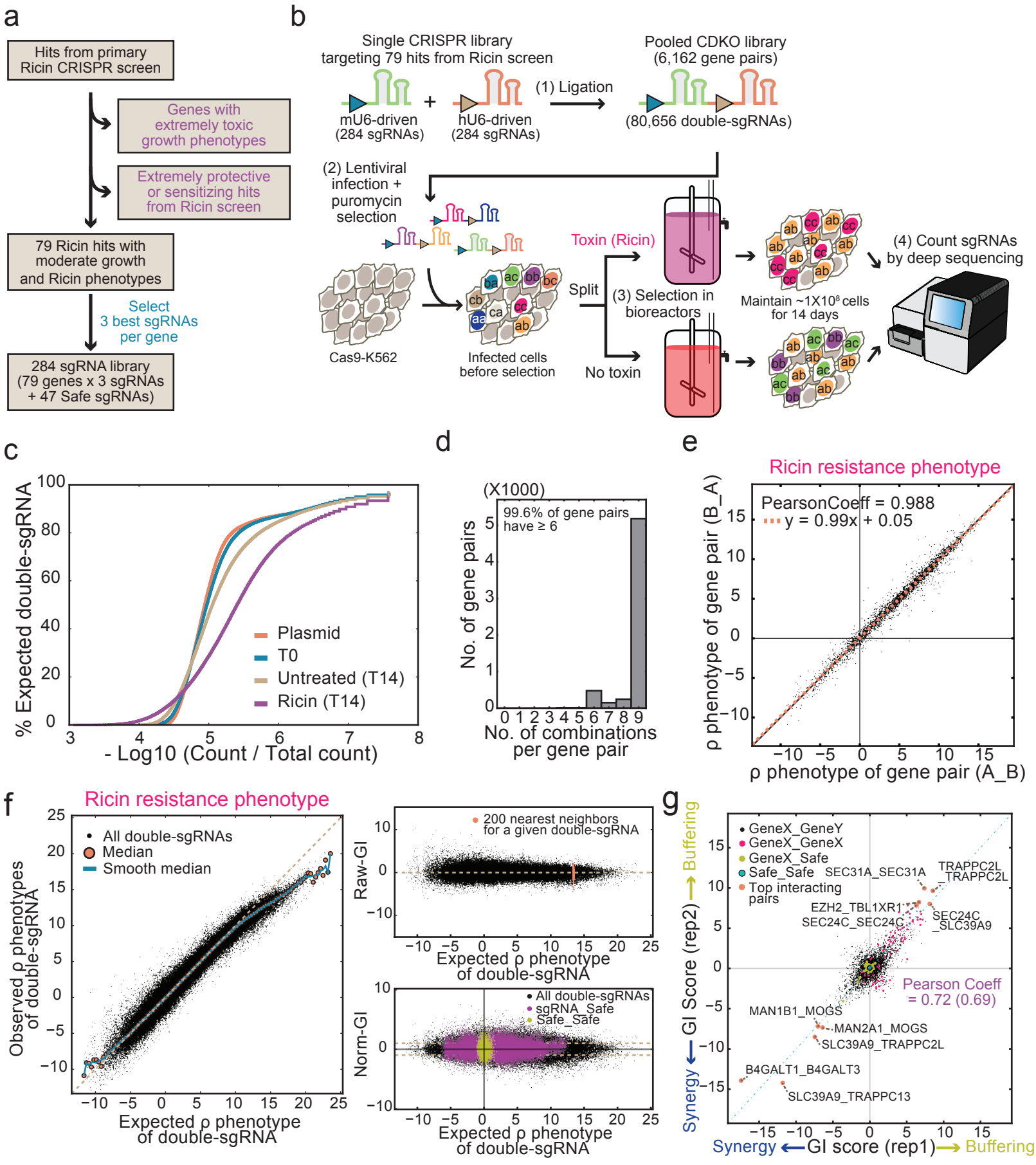
a
Hits from primary Ricin CRISPR screen
Genes with extremely toxic growth phenotypes
Extremely protective or sensitizing hits from Ricin screen
79 Ricin hits with moderate growth and Ricin phenotypes
Select 3 best sgRNAs per gene
284 sgRNA library (79 genes x 3 sgRNAs + 47 Safe sgRNAs)
b
Single CRISPR library targeting 79 hits from Ricin screen
mU6-driven (284 sgRNAs)
hU6-driven (284 sgRNAs)
(1) Ligation
Pooled CDKO library (6,162 gene pairs)
(80,656 double-sgRNAs)
(2) Lentiviral infection + puromycin selection
Cas9-K562
Infected cells before selection
Split
Toxin (Ricin)
No toxin
(3) Selection in bioreactors
Maintain ~1X10^8 cells for 14 days
(4) Count sgRNAs by deep sequencing
c
% Expected double-sgRNA
- Log10 (Count / Total count)
Plasmid
T0
Untreated (T14)
Ricin (T14)
d
(X1000)
No. of gene pairs
99.6% of gene pairs have ≥ 6
No. of combinations per gene pair
e
Ricin resistance phenotype
PearsonCoeff = 0.988
y = 0.99x + 0.05
ρ phenotype of gene pair (B_A)
ρ phenotype of gene pair (A_B)
f
Ricin resistance phenotype
All double-sgRNAs
Median
Smooth median
Observed ρ phenotypes of double-sgRNA
Expected ρ phenotype of double-sgRNA
200 nearest neighbors for a given double-sgRNA
Raw-GI
Norm-GI
sgRNA_Safe
Safe_Safe
g
GeneX_GeneY
GeneX_GeneX
GeneX_Safe
Safe_Safe
Top interacting pairs
SEC31A_SEC31A
TRAPPC2L_TRAPPC2L
EZH2_TBL1XR1
SEC24C_SEC24C
SEC24C_SLC39A9
Pearson Coeff = 0.72 (0.69)
MAN1B1_MOGS
MAN2A1_MOGS
SLC39A9_TRAPPC2L
B4GALT1_B4GALT3
SLC39A9_TRAPPC13
Synergy ← GI Score (rep2) → Buffering
Synergy ← GI score (rep1) → Buffering

Figure S6. Ricin-CDKO screen

(a) Selection of genes modulating ricin-sensitivity and resulting Ricin-CDKO library. **(b)** Schematic of the Ricin-CDKO screen. Infected cells were split into two and one group was treated with 4 pulses of ricin for 14 days, while the other was cultured for 14 days without ricin treatment. **(c)** Cumulative distribution of sequencing reads for double-sgRNAs. **(d)** Histogram plotting the number of double-sgRNAs per gene pair. 99.6% of the 6,063 detected gene pairs have more than 6 double-sgRNA combinations. **(e)** Minimal positional bias in Ricin-CDKO library for **ρ** phenotype. **(f)** Measuring Norm-GIs of double-sgRNAs. Expected and observed **ρ** phenotypes of double-sgRNAs were plotted and deviations from the median line (blue) were processed from Raw-GIs into Norm-GIs as previously done for DrugTarget-CDKO screen. **(g)** t-value-based GI_T scores calculated for **ρ** phenotypes were plotted between two experimental replicates. The 5 most synergistic and buffering pairs by rank-sum of GI_T scores of two replicates are marked in orange dots. The Pearson correlation after same-gene targeting pairs were removed is reported in parentheses.

Figure S7.

a

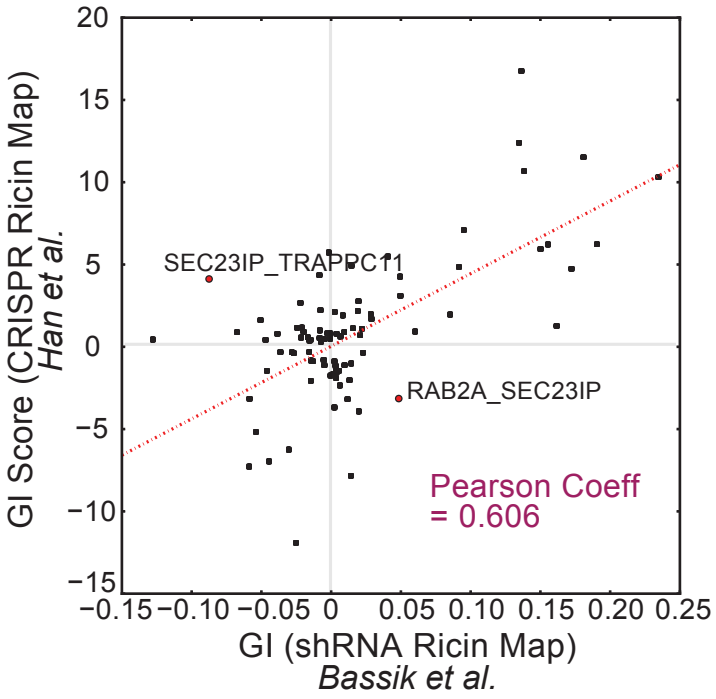

b

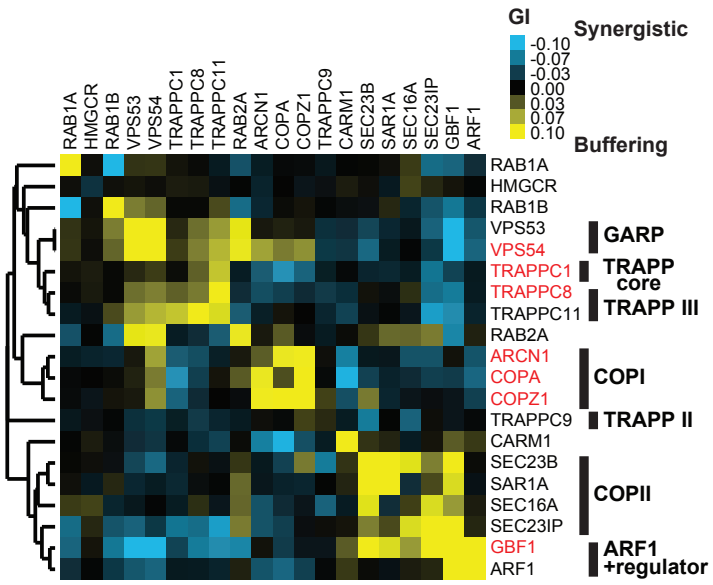

Common complexes from the shRNA-based Ricin Map (*Bassik et al.* Cell, 2013)

c

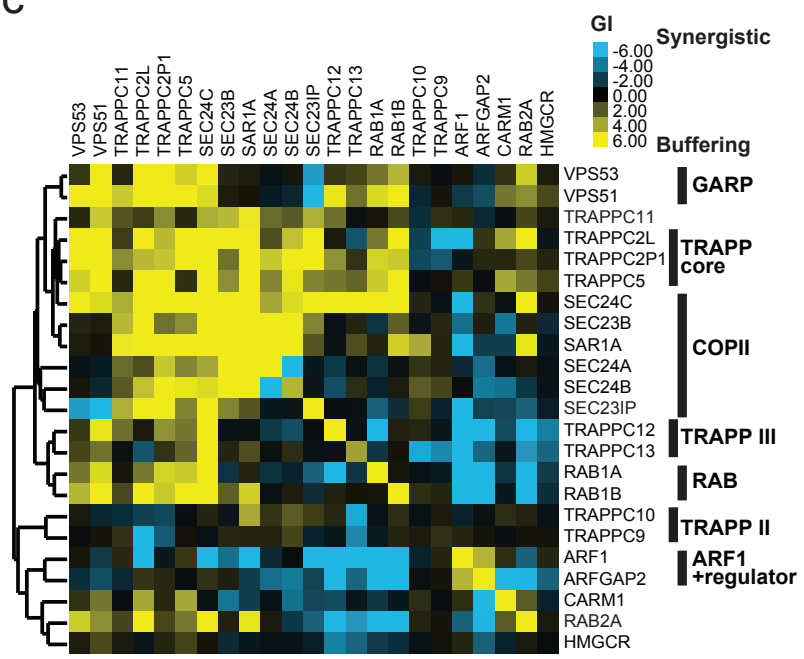

Common complexes from the CRISPR-based Ricin Map (*Han et al.*)

Figure S7. Comparison of a previous shRNA-based ricin GI map with the Ricin-CDKO GI map

(a) Measurement of correlation of genetic interactions between the previously published shRNA-based Ricin GI map[11] and the Ricin-CDKO map for the 91 common interactions present in both maps. GIs are scaled according to the system described in the corresponding manuscript. Two cases of genetic interactions which have opposite signs in the two maps are labeled in the plot. **(b)** Genetic interactions of the common protein complexes and genes between the two maps are used to generate two compact GI maps for comparison. Essential genes are marked in red.

Figure S8.

a

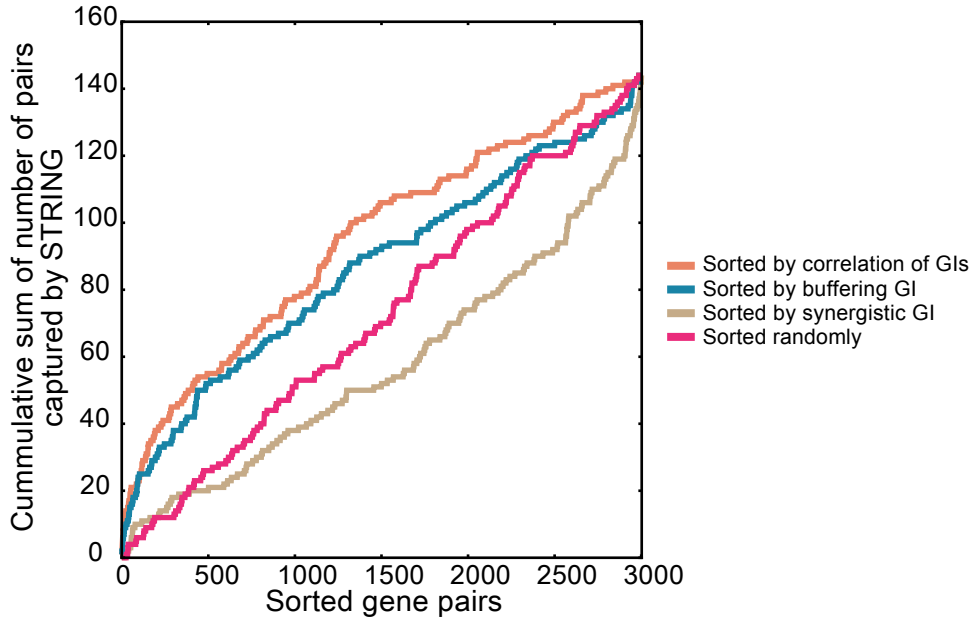

b

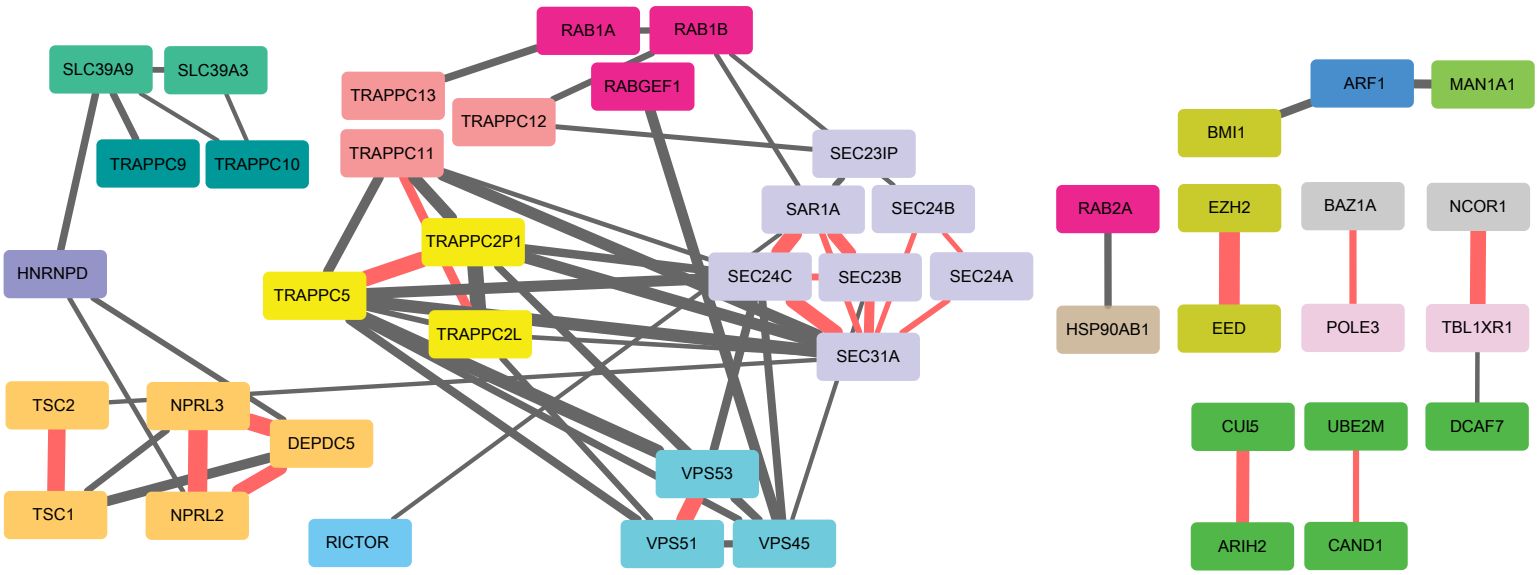

Types of Edges

- Correlation of GIs
- Correlation of GIs captured in STRING

(Width of Edges is determined by GI correlation)

Categories of Nodes

- Mannose-related
- COPII
- Retrograde sorting
- TRAPPCIII
- TRAPPCII
- TRAPPC core
- RAB GTPase
- Endosome to Golgi
- PcG
- Chromatin accessibility complex
- Chromatin remodeling-related
- RNA binding, Splicing
- Solute carrier protein family (Plasma membrane)
- mTOR-related (Protective against Ricin)
- mTOR-related (Sensitizing against Ricin)
- Ubiquitin-related

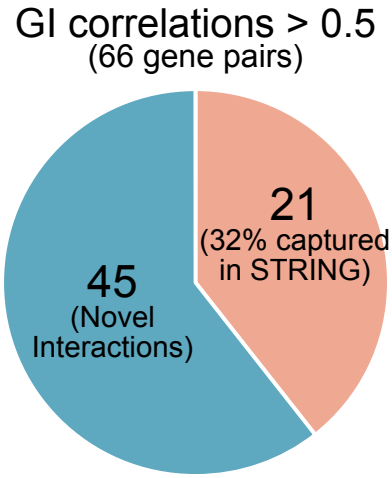

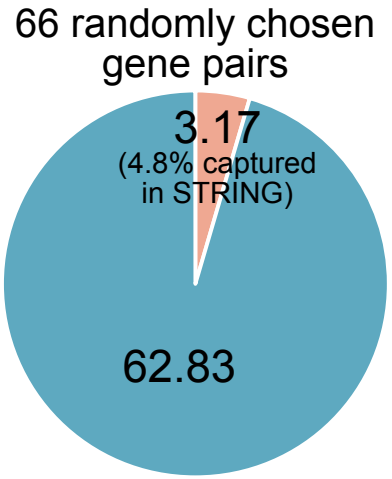

Figure S8. Gene pairs with similar GI profiles are enriched for known protein interactions (see methods)

(a) Data in figure 4d were plotted as AUC (Area Under the Curve). Gene pairs were sorted by the different features of GI map and cumulative sums of the number of STRING interactions identified in the sorted gene pairs were plotted. **(b)** A genetic interaction network of the 66 most correlated gene pairs (GI correlation > 0.5) in terms of GI patterns was generated. Genes are grouped and colored by their biological functions and their known PPIs. Each edge between two genes indicates that they have a correlation of GI patterns over 0.5. A red edge indicates that this gene pair also has known protein interactions reported in STRING. 40% of the 66 gene pairs have reported protein interactions whereas on average, only 5% of 66 randomly selected gene pairs from the Ricin-CDKO map have reported protein interactions in STRING.

Figure S9.

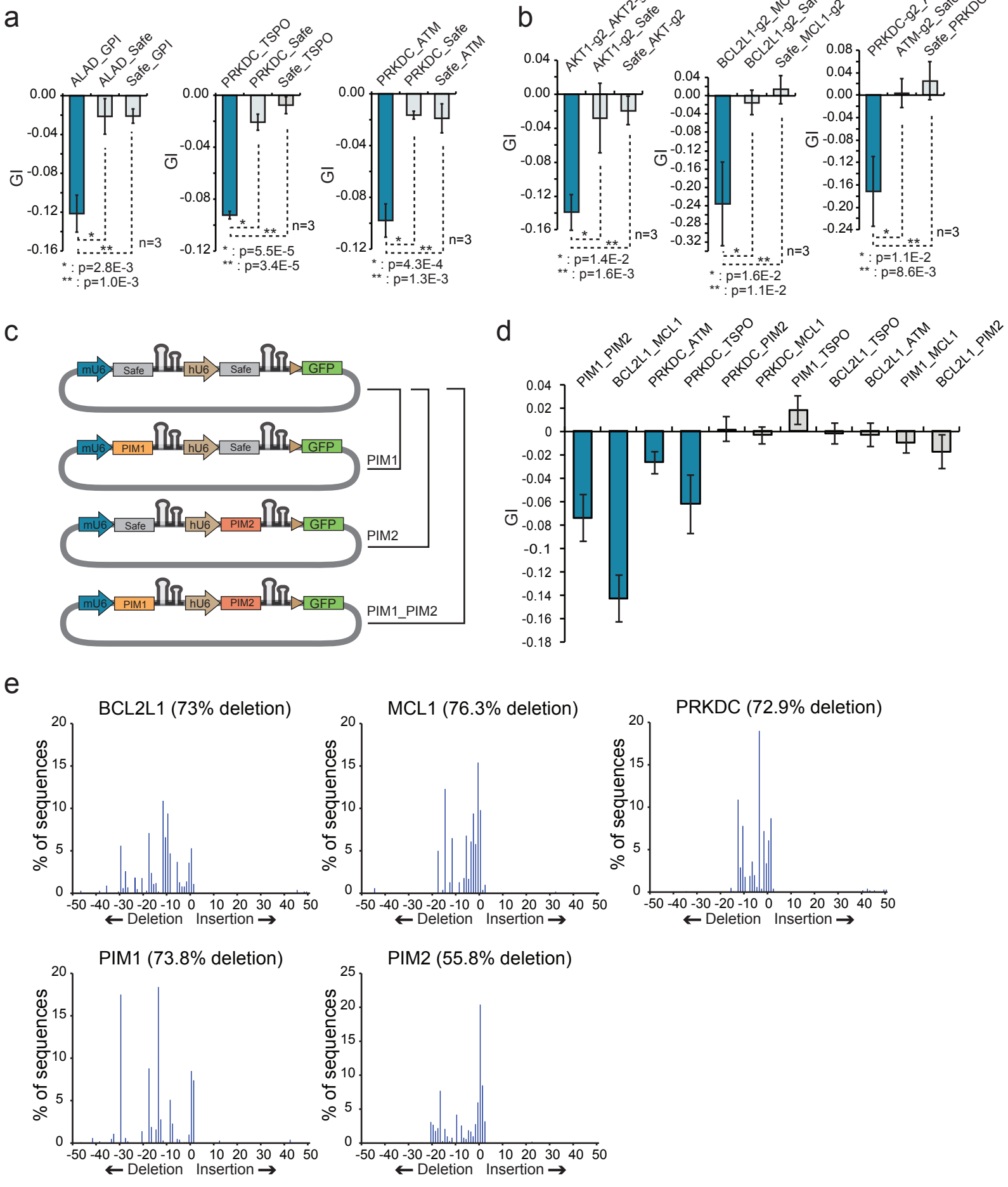
a
ALAD_GPI
ALAD_Safe
Safe_GPI
GI
n=3
* : p=2.8E-3
** : p=1.0E-3
PRKDC_TSPO
PRKDC_Safe
Safe_TSPO
* : p=5.5E-5
** : p=3.4E-5
PRKDC_ATM
PRKDC_Safe
Safe_ATM
* : p=4.3E-4
** : p=1.3E-3
b
AKT1-g2_AKT2-g2
AKT1-g2_Safe
Safe_AKT-g2
* : p=1.4E-2
** : p=1.6E-3
BCL2L1-g2_MCL1-g2
BCL2L1-g2_Safe
Safe_MCL1-g2
* : p=1.6E-2
** : p=1.1E-2
PRKDC-g2_ATM-g2
ATM-g2_Safe
Safe_PRKDC-g2
* : p=1.1E-2
** : p=8.6E-3
c
mU6
Safe
hU6
GFP
PIM1
PIM2
PIM1_PIM2
d
PIM1_PIM2
BCL2L1_MCL1
PRKDC_ATM
PRKDC_TSPO
PRKDC_PIM2
PRKDC_MCL1
PIM1_TSPO
BCL2L1_TSPO
BCL2L1_ATM
PIM1_MCL1
BCL2L1_PIM2
e
BCL2L1 (73% deletion)
MCL1 (76.3% deletion)
PRKDC (72.9% deletion)
PIM1 (73.8% deletion)
PIM2 (55.8% deletion)
% of sequences
← Deletion Insertion →

Figure S9. Validation of synergistic gene pairs with individual sgRNAs

(a) Predicted synergistic gene pairs were validated using individual sgRNAs (using two separate vectors). **(b)** 3 of the synergistic gene pairs were validated using a second pair of sgRNAs. **(c)** Example of GI calculation for individual sgRNA validations using double-sgRNA vector. Double-sgRNA vectors were cloned containing two safe-sgRNAs, one safe-sgRNA and one gene-targeting sgRNA (PIM1_Safe and Safe_PIM2), or two gene-targeting sgRNAs (PIM1_PIM2) and infected into Cas9-expressing K562 cells. Growth phenotypes of single and double gene knockouts are calculated by measuring the depletion of GFP+ cells relative to uninfected cells (PIM1_Safe and Safe_PIM2 for single knockout phenotypes and PIM1_PIM2 for double knockout) from T0 to T7, normalized to Safe_Safe cells. GIs are determined by comparing the observed double knockout phenotype to the expected from the single knockout phenotypes. **(d)** Using the double-sgRNA vector system, synergy was validated for sgRNA pairs predicted to be synergistic (PIM1_PIM2, BCL2L1_MCL1, PRKDC_ATM, PRKDC_TSPO) while sgRNA pairs not predicted to be synergistic did not show synergy in dual-sgRNA retests (PRKDC_PIM2, PRKDC_MCL1, PIM1_TSPO, BCL2L1_TSPO, BCL2L1_ATM, PIM1_MCL1, BCL2L1_PIM2). **(e)** TIDE indel analysis for sgRNAs against indicated genes.

Figure S10.

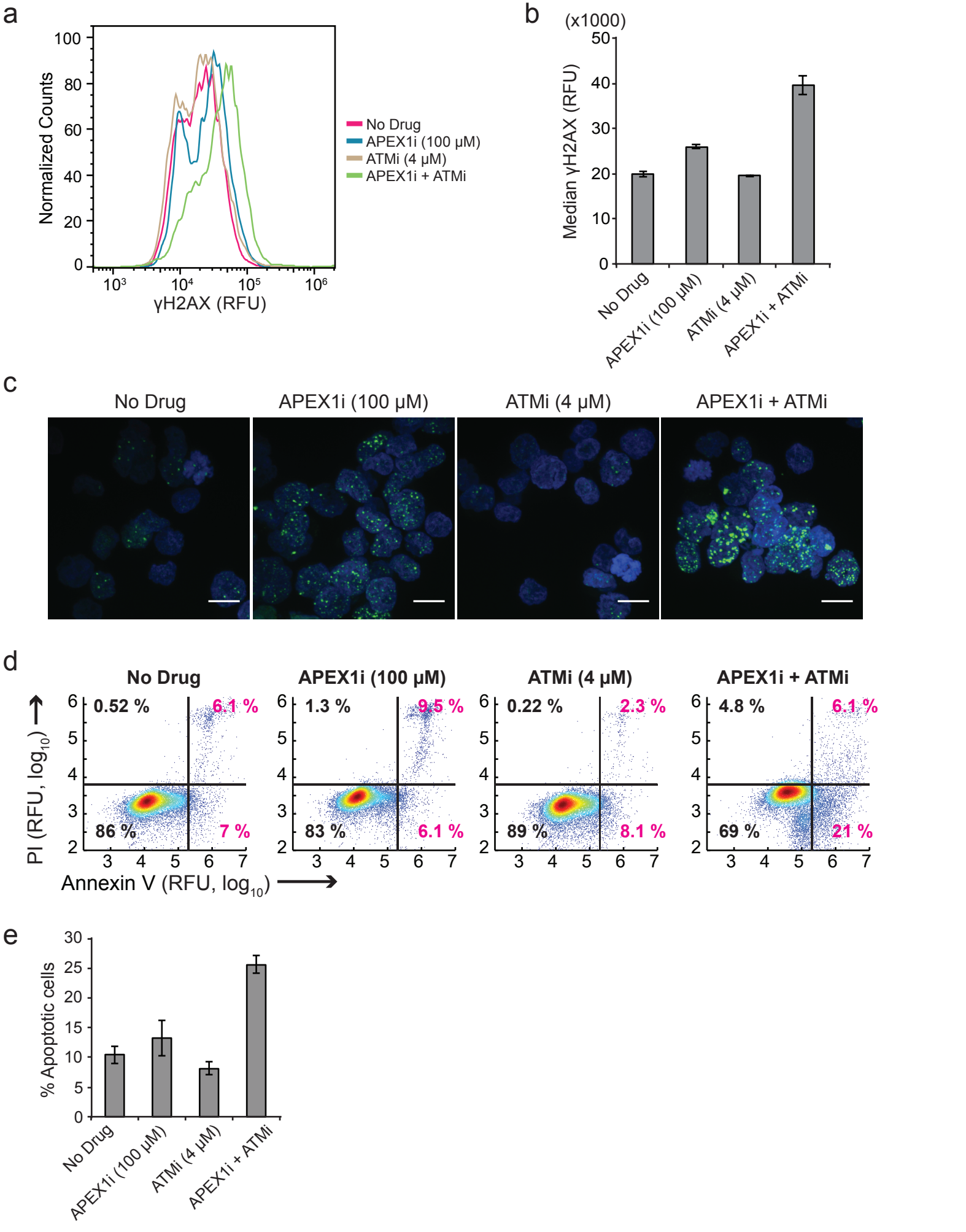
a
Normalized Counts
γH2AX (RFU)
No Drug
APEX1i (100 μM)
ATMi (4 μM)
APEX1i + ATMi
b
(x1000)
Median γH2AX (RFU)
No Drug
APEX1i (100 μM)
ATMi (4 μM)
APEX1i + ATMi
c
No Drug
APEX1i (100 μM)
ATMi (4 μM)
APEX1i + ATMi
d
No Drug
APEX1i (100 μM)
ATMi (4 μM)
APEX1i + ATMi
PI (RFU, log10)
Annexin V (RFU, log10)
0.52 %
6.1 %
86 %
7 %
1.3 %
9.5 %
83 %
6.1 %
0.22 %
2.3 %
89 %
8.1 %
4.8 %
6.1 %
69 %
21 %
e
% Apoptotic cells
No Drug
APEX1i (100 μM)
ATMi (4 μM)
APEX1i + ATMi

Figure S10. Combination APEX1_ATM drug treatment synergistically induces DSBs and apoptosis

(**a-c)** K562 cells were treated with APEX1 (CRT0044876) and ATM (KU-60019) inhibitors for 48 h, fixed, and stained for **γ**H2AX. Cells were analyzed by flow cytometry and representative histograms from each sample are plotted in **a**. Median FL-1 ± SD from 3 replicate cultures are plotted in **b.** Cells were additionally stained with Hoescht and representative images are shown in **c**. Scale bars,10 μm. **(d,e)** K562 cells were treated with indicated drugs for 48 h and assessed by flow cytometry for Annexin V-FITC and propidium iodide (PI) staining. Plots in **d** are representative of three independent experiments and the percentages of Annexin V-positive cells are quantified in **e**.

Figure S11.

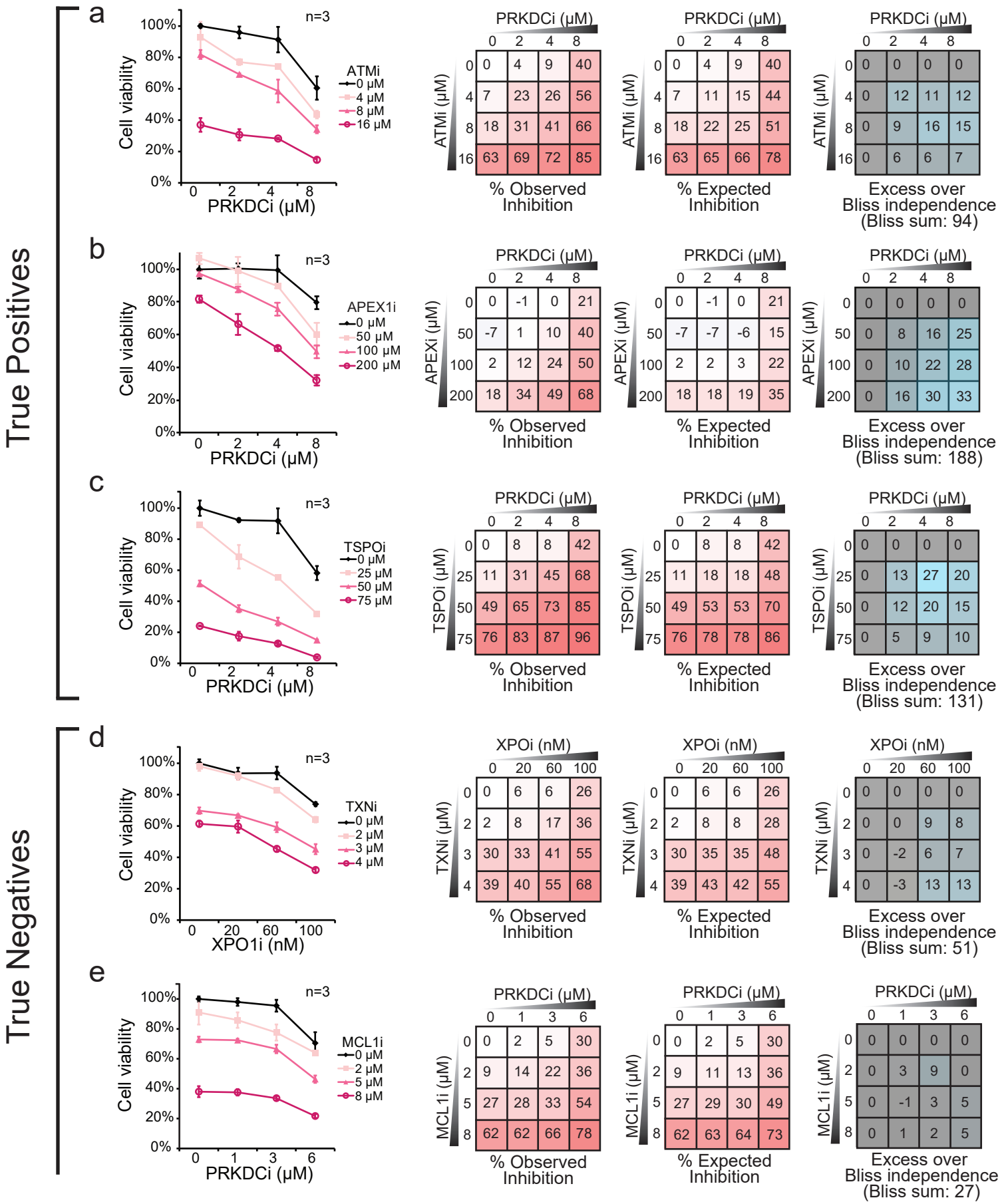
True Positives
True Negatives
a
b
c
d
e
n=3
Cell viability
PRKDCi (μM)
ATMi
0 μM
4 μM
8 μM
16 μM
APEX1i
0 μM
50 μM
100 μM
200 μM
TSPOi
0 μM
25 μM
50 μM
75 μM
XPO1i (nM)
TXNi
0 μM
2 μM
3 μM
4 μM
MCL1i
0 μM
2 μM
5 μM
8 μM
% Observed Inhibition
% Expected Inhibition
Excess over Bliss independence
(Bliss sum: 94)
(Bliss sum: 188)
(Bliss sum: 131)
(Bliss sum: 51)
(Bliss sum: 27)

Figure S11 cont.

True negatives

False positive

False negative

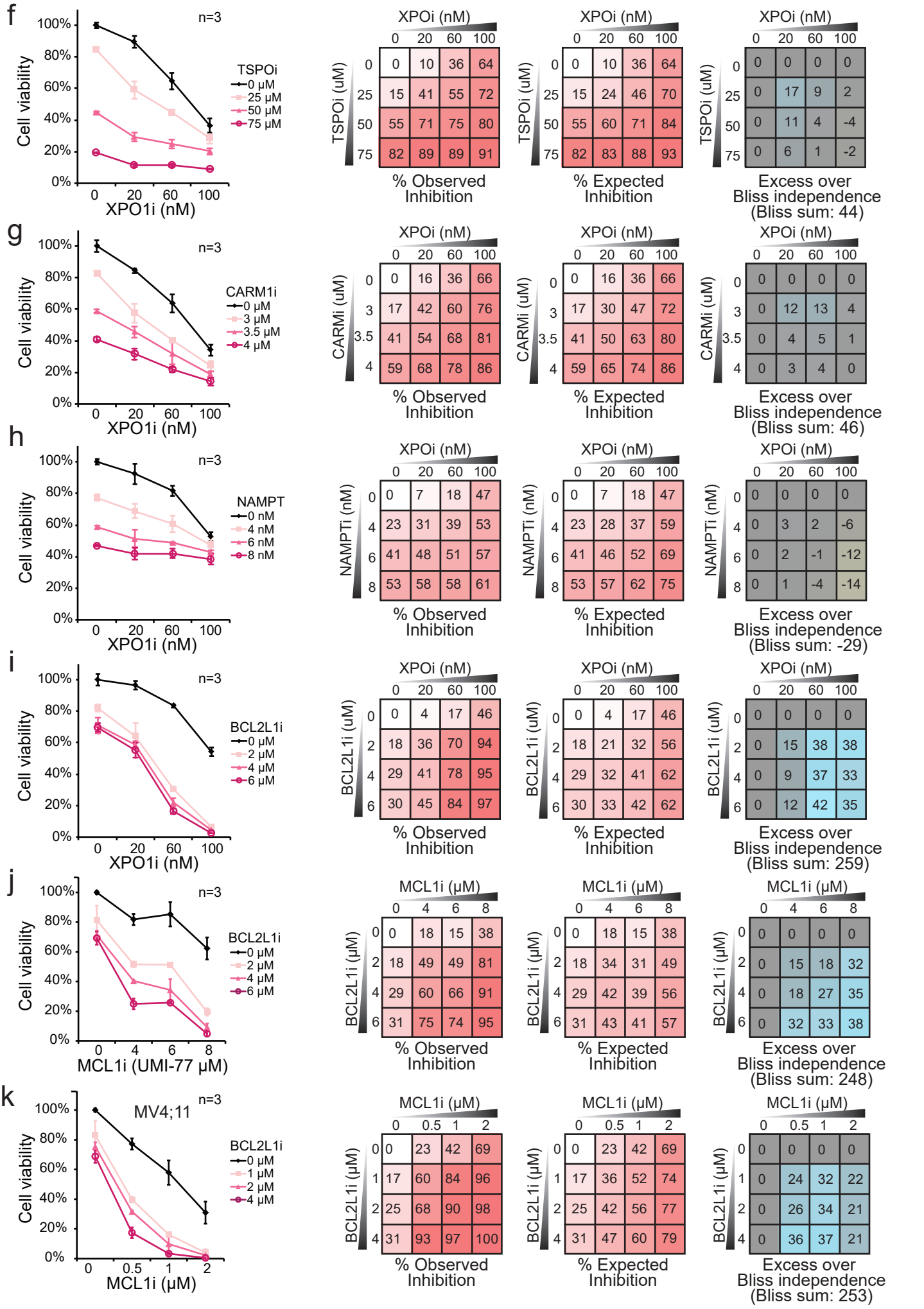

Figure S11. DrugTarget-CDKO genetic interactions predict drug synergy

(a-k) Cell viability and Bliss drug synergy plots for drug pairs in K562 cells **(a-j)** and MV4;11 cells **(k).** Additional true positives are shown in **a-c**: **(a)** ATM (KU-60019) and PRKDC (NU7441), **(b)** APEX1 (CRT0044876) and PRKDC, **(c)** TSPO (PK-11195) and PRKDC. Examples of true negatives are shown in **d-g**: **(d)** TXN (PX-12) and XPO1 (KPT-330), **(e)** MCL1 (A-1210477) and PRKDC, **(f)** TSPO and XPO1, **(g)** CARM1 (1-benzyl-3,5-bis-(3-bromo-4-hydroxybenzylidene)piperidin-4-one) and XPO1. **(h)** NAMPT (FK866) and XPO1 (false positive)**. (i)** BCL2L1 (A-1155463) and XPO1 (false negative). **(j)** The BCL2L1 and MCL1 pair was tested using a different MCL1 inhibitor (UMI-77) and **(k)** in the MV4;11 AML cell line (using A-1155463 and A-1210477)**.**

Figure S12.

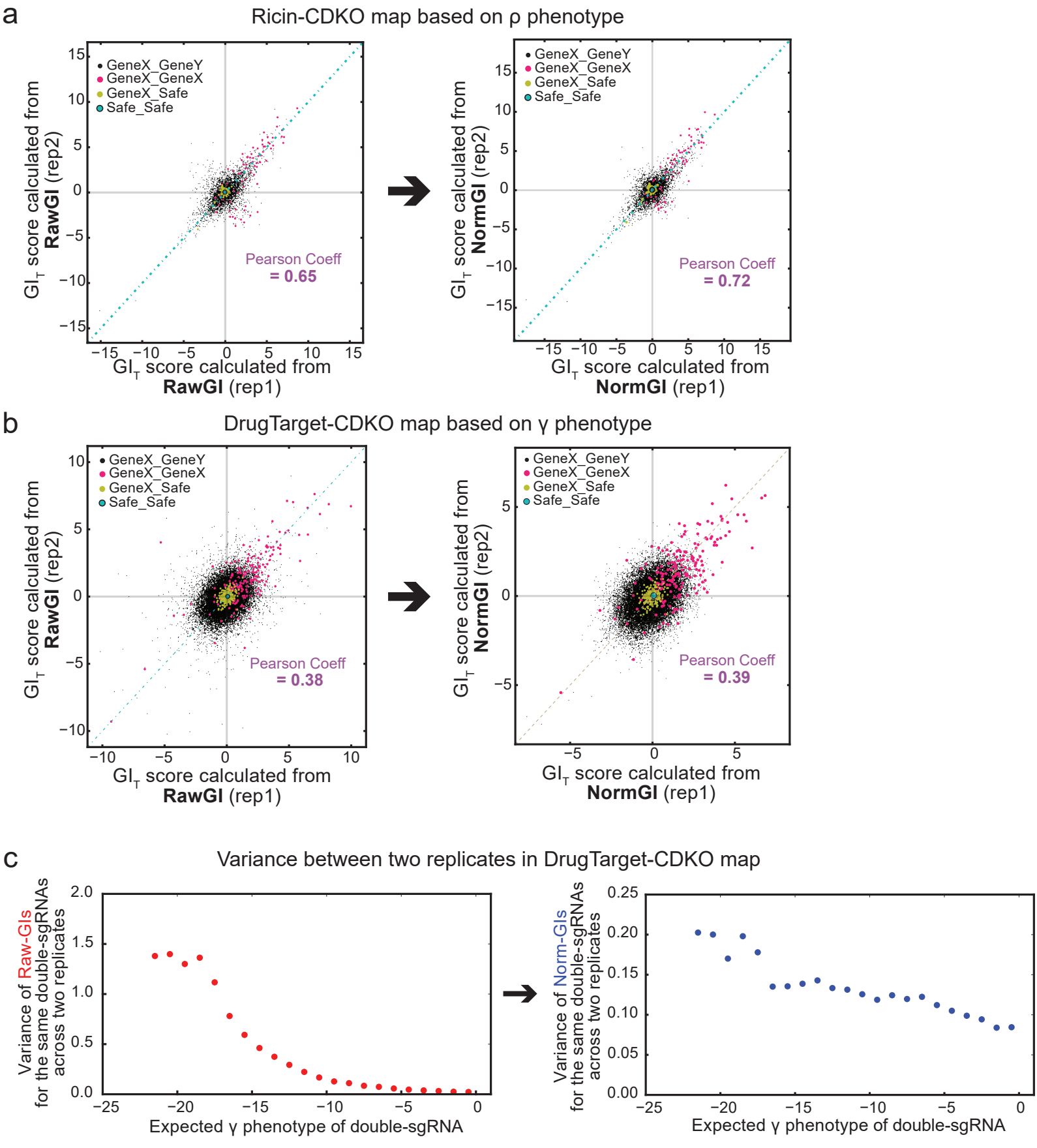
a
Ricin-CDKO map based on ρ phenotype
GeneX_GeneY
GeneX_GeneX
GeneX_Safe
Safe_Safe
Pearson Coeff
= 0.65
GI_T score calculated from RawGI (rep2)
GI_T score calculated from RawGI (rep1)
Pearson Coeff
= 0.72
GI_T score calculated from NormGI (rep2)
GI_T score calculated from NormGI (rep1)
b
DrugTarget-CDKO map based on γ phenotype
Pearson Coeff
= 0.38
Pearson Coeff
= 0.39
c
Variance between two replicates in DrugTarget-CDKO map
Variance of Raw-GIs for the same double-sgRNAs across two replicates
Expected γ phenotype of double-sgRNA
Variance of Norm-GIs for the same double-sgRNAs across two replicates
Expected γ phenotype of double-sgRNA

Figure S12. Normalized GI improves reproducibility of genetic interactions between replicates

(a) GI_T scores calculated from Raw-GI and Norm-GI are compared for the **ρ** phenotype-based Ricin-CDKO map. GI_T scores calculated from Norm-GI show higher correlation between replicates than those from Raw-GI. **(b)** GI_T scores calculated from Raw-GI and Norm-GI are compared for the **γ** phenotype-based DrugTarget-CDKO map. GI_T scores calculated from Norm-GI show slightly higher correlation between replicates than those from RawGI. **(c)** Normalization of GIs improves the uniformity of variance across the range of expected **γ** phenotypes. Variance of Raw-GIs and Norm-GIs for the same guide pairs across two experimental replicates in DrugTarget-CDKO map was measured with respect to the expected **γ** phenotype. Data are binned across the expected **γ** phenotypes (bin number = 22, bin size = 1 pZ) and average variance on each bin is calculated and plotted in the graphs.

SUPPLEMENTARY REFERENCES

1. Shi, J. *et al.* Discovery of cancer drug targets by CRISPR-Cas9 screening of protein domains. *Nat. Biotechnol.* **33,** 661–667 (2015).
2. Zhou, J. *et al.* Dual sgRNAs facilitate CRISPR/Cas9-mediated mouse genome targeting. *FEBS J.* **281,** 1717–1725 (2014).
3. Han, J. *et al.* Efficient in vivo deletion of a large imprinted lncRNA by CRISPR/Cas9. *RNA Biol.* **11,** 829–35 (2014).
4. Chen, X. *et al.* Dual sgRNA-directed gene knockout using CRISPR/Cas9 technology in Caenorhabditis elegans. *Sci. Rep.* **4,** 7581 (2014).
5. Tong, A. H. Y., Lesage, G., Bader, G. D. & Boone, C. Global mapping of the yeast genetic interaction network. *Science* **303,** 808–813 (2004).
6. Costanzo, M. *et al.* A global genetic interaction network maps a wiring diagram of cellular function. *Science* **353,** aaf1420-1-aaf1420-14 (2016).
7. Fischer, B. *et al.* A map of directional genetic interactions in a metazoan cell. *Elife* **4,** 1–21 (2015).
8. Blomen, V. A. *et al.* Gene essentiality and synthetic lethality in haploid human cells. *Science* **350,** 1092–6 (2015).
9. Storey, J. D. & Tibshirani, R. Statistical significance for genomewide studies. *Proc. Natl. Acad. Sci. U. S. A.* **100,** 9440–5 (2003).
10. Morgens, D. W. et al. Genome-scale measurement of off-target activity using Cas9 toxicity in high-throughput screens . Nat. Commun. in press (2017).
11. Bassik, M. C. *et al.* A Systematic Mammalian Genetic Interaction Map Reveals Pathways Underlying Ricin Susceptibility. *Cell* **152,** 909–922 (2013).